Spatial Variations in Vegetation Fires and Carbon Monoxide Concentrations in South Asia

Krishna Prasad Vadrevu, Kristofer Lasko and Chris Justice

Abstract Vegetation fires are an important source of air pollution in several regions of the world including Asia. An important question with respect to satellite retrievals of air pollutants is "how well do they capture temporal and spatial variations and how well do they relate to episodic events such as fires?" We addressed this question using MOPITT surface CO and MODIS fire retrievals. We also evaluated MODIS aerosol optical depth (AOD) as well as small mode aerosol fraction (SMAF) variations in relation to fire seasonality. Results from temporal analysis (2003–2012) of fires in Asia suggested 22 % of all fires occurring in Myanmar, followed by India (20.91 %), Indonesia (18.31 %), Thailand (9.42 %), etc. Fire frequencies were highest in northeast India and Southeast Asia countries. Further, we observed significant spatial variation and seasonality in fires in Southeast Asia. In the northern Southeast Asia, the peak fire season was during January–March whereas in the south, the fires peak is from August through October. AOD followed a similar trend as that of fires, however, small mode aerosol fraction showed some discrepancies. Locally weighted regression yielded good results between vegetation fires and CO emissions. Results showed that areas with high vegetation fires were also areas of high CO emissions, with highest spatial correlation during the month of March. Among the fire counts and FRP, the correlations varied for individual months, however, both showed significant ($P < 0.001$) positive correlations suggesting that either of them can be used as predictor of CO concentrations. Locally weighted regression maps revealed how the relationship between fire counts versus CO and FRP versus CO change across time and space. The study captures the influence of vegetation fires on CO pollution in Asia using satellite data.

Keywords Vegetation fires · MODIS · MOPITT · Satellites · Carbon Monoxide · South Asia

K. P. Vadrevu (✉) · K. Lasko · C. Justice
Department of Geographical Sciences, University of Maryland, College Park, USA
e-mail: krisvkp@umd.edu

P. K. Srivastava et al. (eds.), *Remote Sensing Applications in Environmental Research*, Society of Earth Scientists Series, DOI: 10.1007/978-3-319-05906-8_8,

1 Introduction

Vegetation fires have significant regional and global impacts on the tropospheric chemistry and air pollution. In addition to slash and burn from forests (Prasad et al. 2008), agricultural residue burning to clear crop waste is another major source of air pollution in the Asian region (Li et al. 2010; Miettinen et al. 2011; Vadrevu et al. 2011, 2013). Historically, fires in the Asian region attracted international attention during 1997/1998 when a severe haze episode occurred due to wildfires in Indonesia. In the Indonesia, the area burned during 1997/1998 is estimated at 9.7 million hectares of forest and non-forest land, with some 75 million people affected by smoke, haze, and the fires themselves (Murdiyarso and Adiningsih 2007). The haze covered the entire area of Sumatra and Kalimantan and extended up to Malaysia, Singapore and the Southern part of Thailand due to long-range transport (Page et al. 2009; Bonnet and Garivait 2011). Impacts included damage to health, loss of life, property and reduced livelihood options. The economic costs were estimated to exceed 9 billion USD (Dennis et al. 2005). The impacts of the atmospheric pollution on health, transport and tourism, largely were borne by Indonesia, Brunei Darussalam, Singapore and Malaysia (Radojevic 2003). Fires in the Asian region were also associated with carbon emissions, environmental and economic losses (Vadrevu and Badarinath 2009; Vadrevu et al. 2010). For example, recent estimates suggest that the peat lands of southeast Asia cover approximately 250,000 km^2 (Page et al. 2011) and represent an immense reservoir of fossil carbon (Page et al. 2002; Jaenicke et al. 2008). CO_2 emissions from Peat fires are estimated at about $\sim$30 % of the global CO_2 emissions (Hooijer et al. 2012). Similarly, in India, the Himalayan forest fires during 1995 consumed nearly 6 Mha and caused huge economic losses (Kimothi and Jadhav 1998). The regular agricultural residue burning events that occur till date in the Punjab province of India were shown to cause enormous pollution problems including enhancing of direct radiative forcing in the Indo-Ganges region (Ramanathan and Carmichael 2008; Vadrevu et al. 2010). Likewise, Chan et al. (2000) from the ozonesonde profiles, fire count, Carbon monoxide (CO) data and back air trajectory analysis showed that biomass burning emissions in the south east Asia are the source of ozone enhancement in the lower troposphere in springtime at Hong Kong. More examples of the impacts of fires on the local environment specific to Asia can be found in Chan et al. (2000), Hsu et al. (2003), Ramanathan et al. (2005), Lau et al. (2010), Vadrevu et al. (2011), (2012a, b), Fu et al. (2012), etc. In addition to these climate impacts, adverse health impacts have been reported due to biomass burning pollutants. The aerosols released from biomass can cause asthma, bronchitis, emphysema, or pneumonia (Seaton et al. 1995; Nawahda et al. 2012). Carbon monoxide released from biomass burning can damage the respiratory system by interfering with the blood's ability to absorb oxygen (Suji et al. 1990). Considering the climate and health impacts of vegetation fires, accurate information on fires (location, frequency, extent, seasonality) is necessary to make

informed decisions on the fire management and resulting ecological and air pollution impacts.

Links between biomass burning and air pollution need thorough investigation. In particular, CO is one of the dominant greenhouses released due to incomplete combustion of either fossil fuels or biomass. CO also has a relatively long atmospheric lifetime on the order of months and strongly influences the abundance of the OH radical, thereby altering the lifetime of methane and other greenhouse gases (Montzka et al. 2011). It is estimated that biomass burning accounts for about 331.1–351.52 Tg CO/yr with large inter-annual variations (van der Werf et al. 2006; Kaiser et al. 2012). Surface CO measurements over South Asia are extremely sparse and measurements of the vertical distribution of CO do not exist over the region (Kumar et al. 2013). Specific to the Asian region, biomass burning contributes to ~62–420 Tg C/yr (Streets et al. 2003; Hoelzemann et al. 2004; Van der Werf et al. 2006). Recently, Chang and Song (2010) using L3JRC and MCD45A1 satellite burned area products and following the Seiler and Crutzen approach (1980) estimated ~8.6 and 6.3 Tg CO/yr from forest/shrub and grassland burning compared to an earlier estimate of 35 Tg CO/yr (Streets et al. 2003). Chang and Song (2010) using satellite data also estimated that crop residue burning accounts for about 2.9–3.0 Tg/yr compared to 35 Tg CO/yr (Streets et al. 2003). These estimates clearly suggest significance of vegetation fires in releasing CO and also some discrepancies in the CO emission estimates.

The use of satellite remote sensing for characterizing the greenhouse gases in the troposphere is a science that has developed within the past twenty years (Burrows et al. 2011). For air quality mapping and monitoring, direct measurements of CO from space might resolve some uncertainties in emission estimates. CO has a strong absorption in the thermal infrared (4.7 μm) and shortwave infrared (2.3 μm) region of the spectrum. Based on this a number of space-borne instruments have been measuring tropospheric CO globally over the past decade, including MOPITT, SCIAMACHY, AIRS, ACE-FTS TES and IASI and as a result, the measurement of trace gas emissions from satellites has improved considerably (Kopacz et al. 2010). An important question with respect to satellite retrievals of air pollutants is "how well do they capture temporal and spatial variations and how well do they capture emissions from episodic events such as fires?" In this work, we address this question through analyzing the spatial variability in CO and vegetation fires in the Asia using MOPITT and MODIS datasets. Nine years of vegetation fire data has been used in conjunction with MOPITT data to characterize fire–CO relationships spatially and temporally. We focused on the below questions:

(a) What is the influence of vegetation fires on CO emissions in the Asian region? (b) How do active fires and fire radiative power (FRP) relate to CO emissions? (c) Which product, active fires or FRP better relates to CO emissions? (d) What are the spatial patterns in correlation strength between vegetation fires and CO emissions in the Asian region? (e) Does the correlation strength vary among different months, if so by how much? (f) How does aerosol optical depth and aerosol small mode fraction vary in relation to fires and how do they relate to CO?

In this study, in addition to fire counts, we also used FRP as a predictor of CO as FRP has been shown to directly relate to fire intensity and biomass consumption (Wooster et al. 2004; Ichoku et al. 2008). Thus, it was hypothesized that FRP should be well correlated with surface CO emissions retrieved from the MOPITT datasets.

2 Data Sets and Methodology

2.1 Vegetation Fires

For characterizing the vegetation fires in the region, we used daily active fire detections from the MODIS instruments onboard the Aqua and Terra satellites. The two MODIS sun-synchronous, polar-orbiting satellites pass over the Equator at approximately 10:30 a.m./p.m. (Terra) and 1:30 p.m./a.m. (Aqua) with a revisit time of 1–2 days. MODIS Advanced Processing System (MODAPS) processes the resulting data using the enhanced contextual fire detection algorithm (Giglio et al. 2003) combined into the Collection 5 Active Fire product. For this study, we analyzed the data from 2003–2012. The fire data are at 1 km spatial resolution at nadir; however, under ideal conditions it can detect flaming fires as small as 50 m^2. FRP is the rate of fire energy released per unit time, measured in megawatts (Kaufman et al. 1998). The MODIS algorithm for FRP is calculated as the relationship between the brightness temperature of fire and background pixels in the middle infrared (band center near 4 μm). It is given as (Kaufman et al. 1998),

$$FRP = 4.34 \times 10^{-19}(T_{MIR}^{8} - T_{bgMIR}^{8})$$

where FRP is the rate of radiative energy emitted per pixel, 4.34×10^{-19} MW km^{-2} K^8 is the constant derived from the simulations, T_{MIR} (Kelvin) is the radiative brightness temperature of the fire component, T_{bgMIR} (Kelvin) is the neighboring non-fire background component, and MIR refers to the middle infrared wavelength here, 3.96 μm. In this study, we utilized the Collection 5 Terra and Aqua monthly climate modeling grid datasets (MOD14CMH/MYD14CMH) that represent cloud and overpass corrected fire pixels data along with the mean FRP data.

2.2 MOPITT CO Retrievals

For characterizing the geographical extent of CO pollution, we used the MOPITT CO datasets. MOPITT instrument, launched in December 1999 aboard the NASA EOS Terra satellite, is a thermal nadir-viewing gas correlation radiometer (Drummond 1992; Deeter et al. 2003). It measures CO at a spatial resolution of

22 km × 22 km. Terra has a near polar sun-synchronous orbit with a descending equator crossing time of approximately 10:30 a.m. local time (ascending 10:30 p.m.). CO profiles are retrieved from radiance measurements in the thermal infrared channel at 4.7 mm (Deeter et al. 2003) and MOPITT achieves a global coverage within 3 days. We used the Version 4 Level 3 (L3) product which includes CO concentrations, averaging kernels and error co-variances at 10 pressure levels retrieved in linear space in surface, 900, 800, 700, 600, 500, 400, 300, 200, and 100 hPa) (Deeter et al. 2009). Of these columnar data, we used only surface data (~900 hPa) to infer fire–CO variations. Retrieved CO total columns are calculated by integrating the retrieved mixing ratio profile and each retrieval 'level' corresponds to a uniformly weighted layer immediately above that level. For example, the surface-level retrieval product corresponds to the mean volume-mixing ratio over the layer between the surface and 900 hPa. For CO vertical profiles, estimated errors are available in the error field of the "retrieved CO Mixing ratio profile" and "retrieved CO Surface mixing ratio" variables of the MOPITT files. These values represent the cumulative error from smoothing error, model parameter error, forward model error, geophysical noise, and instrument noise (Deeter and MOPITT team 2009) contributing to ~20–30 % uncertainty with 5 % difference in the monthly mean CO. A detailed review on the use satellite datasets for characterizing CO emissions from biomass burning has been reviewed by Monks and Beirle (2011).

2.3 Aerosol Optical Depth (AOD) and Aerosol Small Mode Fraction (SMAF)

We used the MODIS Collection 5.1 Terra (MOD08_M3) AOD at 550 nm (Remer et al. 2005; Levy et al. 2007) level 3 monthly product for characterizing the variations in relation to fires. The aerosol properties are derived by the inversion of the MODIS-observed reflectance using pre-computed radiative transfer look-up tables based on aerosol models (Remer et al. 2005; Levy et al. 2007). In addition, we also used the aerosol small/fine mode AOD fraction (SMAF) data at 500 nm for spatial variations in fire affected regions. SMAF is the ratio of small mode optical depth (thickness) to the total AOD.

2.4 Spatial Gridding, Ordinary Linear Regression (OLR) and Locally Weighted regression

We spatially gridded the vegetation fire data at 10-min intervals (~9.3 km^2 cells) to infer fire frequencies. We calculated the fire frequency per grid cell to see how many times an individual cell is impacted by fires over a period of nine years

(2003–2011). First, we summed the total number of fires reported by each data record $N_{k,m}^{MODIS,A,T}$ falling within a grid box, k, for each month (m) taking daily observations of Aqua and Terra MODIS fire counts, $M_{k,m}$ the number of months of MODIS observations (2003–2011). Then, we determined the frequency of fire per grid cell as $N_{k,m}^{MODIS,A,T} \Big/ M_{k,m}$ for each month. The resulting map thus had a range of values from 0–9, with zero values suggesting that no fires occurred during the assessed period while a maximum of 9 suggesting that the pixel is impacted by fires every year starting (2003–2011). In addition to fire frequencies, for the same time period we also gridded the FRP. For CO, for spatial gridding, we used 0.5 × 0.5 degree resolution, as the MOPITT CO original data was in 22 × 22 km^2. Corresponding fire counts and FRP data were retrieved from MODIS climate modeling grid product (CMG) (Giglio et al. 2006). Fire counts and FRP data were then used in a regression framework for assessing the relationships using an ordinary linear regression as well as locally weighted regression.

An ordinary linear regression can be expressed as (Huang and Leung 2002),

$$Y_i = a_0 + \sum_{k=1}^{P} a_k x_{ik} + \theta_i \quad i = 1, \ldots n$$

where Y is the dependent variable and is represented as a linear combination of independent variables X_k, k = 1, 2, P; a_0, a_1…, a_p are the parameters and θ_i are independent normally distributed error terms with zero mean and constant variance. In the OLR model, the parameters are assumed to be the same across the study region, which may not be true because different locations might have different parameters.

In this study, to better account for the spatial variations and relationships (spatial non-stationarity) in Fire/FRP versus CO, locally weighted regression also known as geographically weighted regression has been used (Cleveland and Devlin 1988; Fotheringham et al. 2002). The locally weighted regression accounts for the spatial heterogeneity in responses to variables by estimating separate regression for each sample observation including the location of interest and other spatially weighted observations. The weights represent the adjacency effects for neighboring locations within a specified distance (or bandwidth). Following the assumption that more proximate locations are more alike, the weights decay with distance following a bi-square decay function for an adaptive kernel. When regression points and observation points are the same, one regression is estimated for each observation, allowing parameter estimates to vary across the sample space. The locally weighted regression model is specified as

$$y_i = \beta_{i0} + \beta_{i1} x_{i1} + \beta_{i2} x_{i2} + \cdots + \beta_{ik} x_{ik} + \varepsilon_i; \varepsilon_i \sim N(0, \sigma^2), \quad i = 1, 2, \ldots n,$$

Table 1 Annual fire counts for different countries in South Asia obtained through averaging eleven years (2002–2012) of MODIS aqua and terra datasets

Country	Fire counts	% occurrence
Afghanistan	234	0.074
Bangladesh	3,114	0.980
Bhutan	223	0.070
Brunei	32	0.010
Cambodia	25,921	8.156
India	66,479	20.918
Indonesia	58,198	18.312
Laos	31,759	9.993
Malaysia	4,334	1.364
Maldives	0	0.000
Nepal	2,268	0.714
Pakistan	7,104	2.235
Philippines	4,475	1.408
Myanmar	67,503	21.240
Sri Lanka	1,289	0.406
Thailand	29,959	9.427
Vietnam	14,907	4.691
Singapore	6	0.002

Percent values are also shown

where, the 'I' subscripts on the parameters indicate that there is a separate set of (k + 1) parameters for each of the n-observations. The parameter estimates are given as,

$$\hat{\beta}_i = (X^i W_i X)^{-1} X' W_i Y; \quad i = 1, 2, \ldots n$$

where, W_i is the n × n weight matrix whose off-diagonal elements are zero land the diagonal elements are the weights of each observation relative to I, i.e., W_i = diagonal (w_{i1}, w_{i2}, … w_{in}). The optimal bandwidth distance used in each observations regression is determined by the Akaike Information Criterion (AIC) test. The results obtained from this approach were reported in addition to OLR results.

3 Results and Discussion

Annual MODIS fire counts obtained through averaging the data from 2002–2012 for the south Asian countries are shown in Table 1 along with the percent contribution. Of the different countries, 22 % of all fires occurred in Myanmar, followed by India (20.91 %), Indonesia (18.31 %), Thailand 9.42 %), Cambodia (8.15 %), etc. Temporal statistics of fire counts for different countries are shown in Fig. 1a, b. Of the different years, 2004 had the highest number of fire counts in the Asian region with 406,627 fires, 2009 (367,534 fires), 2007 (358,433) and others. Spatial patterns in MODIS Aqua and Terra fire occurrences for the period of

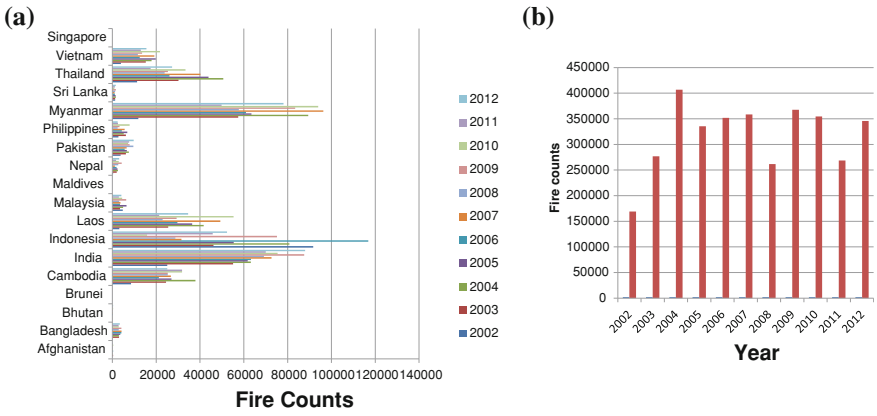

Fig. 1 **a** MODIS aqua and terra fire counts for individual countries (2002–2012). **b** MODIS total fire counts for different years

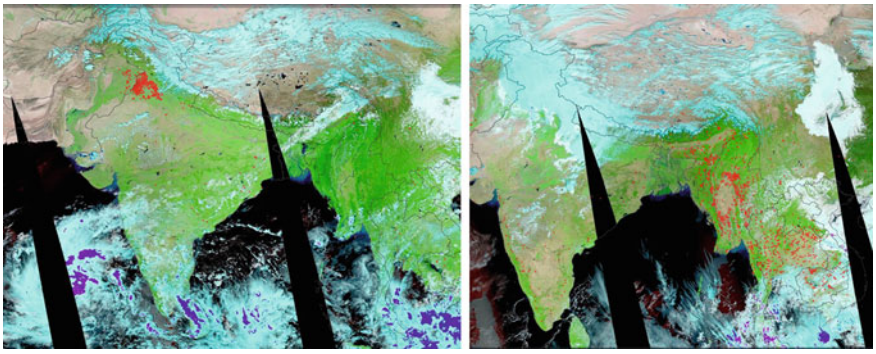

Fig. 2 **a** Fires over Punjab, India on October 22nd, 2012 and southeast Asia on May 11th, 2012. **b** MODIS aqua and terra fires were overlaid on MODIS aqua surface reflectance product (7:2:1)

October agricultural residue burning in Punjab and May forest burning for the study region are shown in Fig. 2a, b. The images clearly suggest significant amount of spatial variation in fires in Asia. The peak burning season is March with 3,702 fire counts per 10-min grid cells with a mean FRP (MW) of 226.28 MW (Figs. 3, 4). Although April recorded fewer fires (2,622) per 9.3 km^2 grid cell, it had a higher mean FRP (226.28 MW) than March (152.53 MW) suggesting relatively higher intensity (Fig. 4).

Fire frequency map calculated using nine years of MODIS data for the month of March at a 9.3 km^2 gridded data is shown in Fig. 5. Results clearly suggested highest fire frequencies in northeast India and southeast Asia countries, mainly Myanmar, Laos, Thailand, Vietnam, etc. Further, we observed significant spatial variation, seasonality as well as fire frequencies in Southeast Asia countries (Fig. 6a, b). For example, in the northern part of southeast Asia, the peak fire

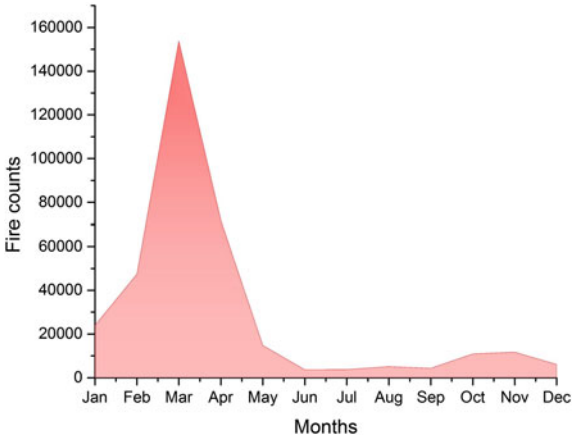

Fig. 3 MODIS aqua and terra monthly fire counts (averaged from 2002–2012)

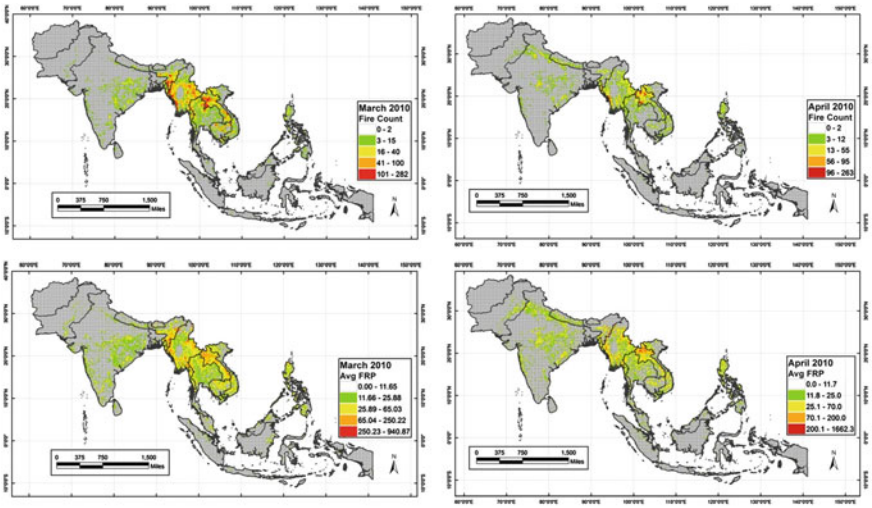

Fig. 4 MODIS fire counts and FRP (MW) aggregated at 9.3 km^2 grid cells (2010)

season was observed during January–March, especially in the region covering Cambodia, Laos PDR, Myanmar, Thailand and Vietnam; whereas in the southern southeast Asian countries of Indonesia and Malaysia, the peak burning season is from August through October (Fig. 6a, b). The fire seasonality has a significant impact on air pollution including CO concentrations.

CO data has been analyzed corresponding to fire counts in grid cells. CO concentrations peaked during March reaching above 700 ppbv during that month followed by April (625.6 ppbv). During winter, December had the highest CO concentrations (548.8 ppbv), followed by November (423.6 ppbv) (Table 2).

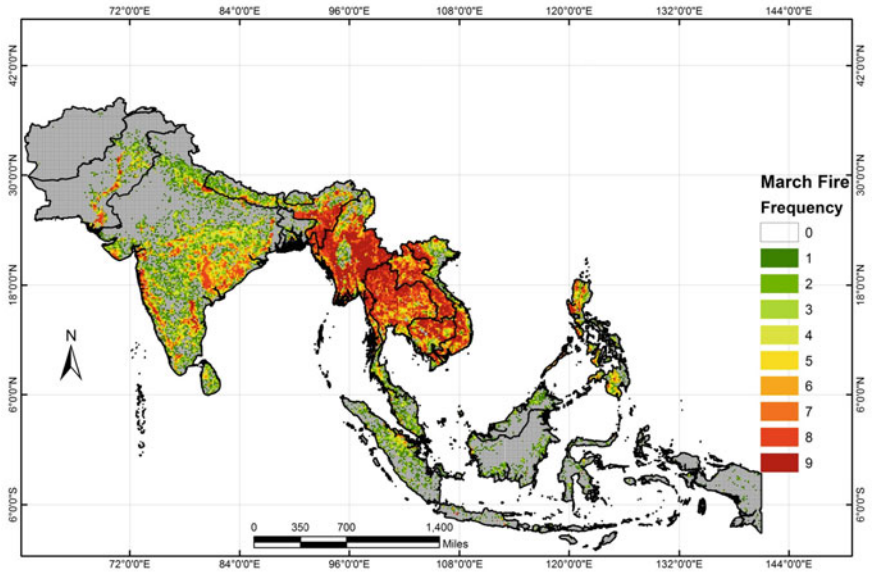

Fig. 5 Fire frequency per 9.3 km^2 grid cells during the month of March (2003–2011)

Spatial patterns suggested highest CO concentrations in the northeast India and Southeast Asia countries around 80–90° latitude and 20–30° longitude (Figs. 7, 8). In conjunction with the MODIS fire counts, AOD and SMAF showed temporal variations (Fig. 8). The seasonal trend in monthly average AOD suggested a steady increase of AOD from January (0.17) with a peak in March (0.61) and April (0.49) during summer and a second peak during October (0.22). Fine mode biomass burning aerosols were found to be quite high during Jan–March and also in November (Fig. 8). Although the Drastic increase in November SMAF coincides with agricultural residue burning (Gadde et al. 2011; Vadrevu et al. 2011), the increase could not be explained by fire counts and FRP alone (Fig. 8). One of the recent studies suggests that in addition to emission sources, relative humidity explains large increases or decreases in the SMAF (Bose 2012). Thus, more intense study is needed to evaluate SMAF variations in relation to meteorological parameters.

To assess the correlation strength between fire counts versus CO and also FRP versus CO, we tested the locally weighted regression approach in addition to OLR. We opted for locally weighted regression as the standard OLR approach estimates one fixed global set of regression coefficients. However, spatially clustered data such as fires and the resulting emissions (CO) could have residuals that can be either over or underestimated. In standard approaches, the ensuing spatial correlation caused by the underlying heterogeneity in the regression coefficients would be indistinguishable from standard spatial error correlation that is generated by clustered data (Fotheringham et al. 2002). Locally weighted regression can account for such errors and the results from fire counts versus CO and FRP versus CO for the peak biomass burning months were shown in (Fig. 9a, b and Table 3).

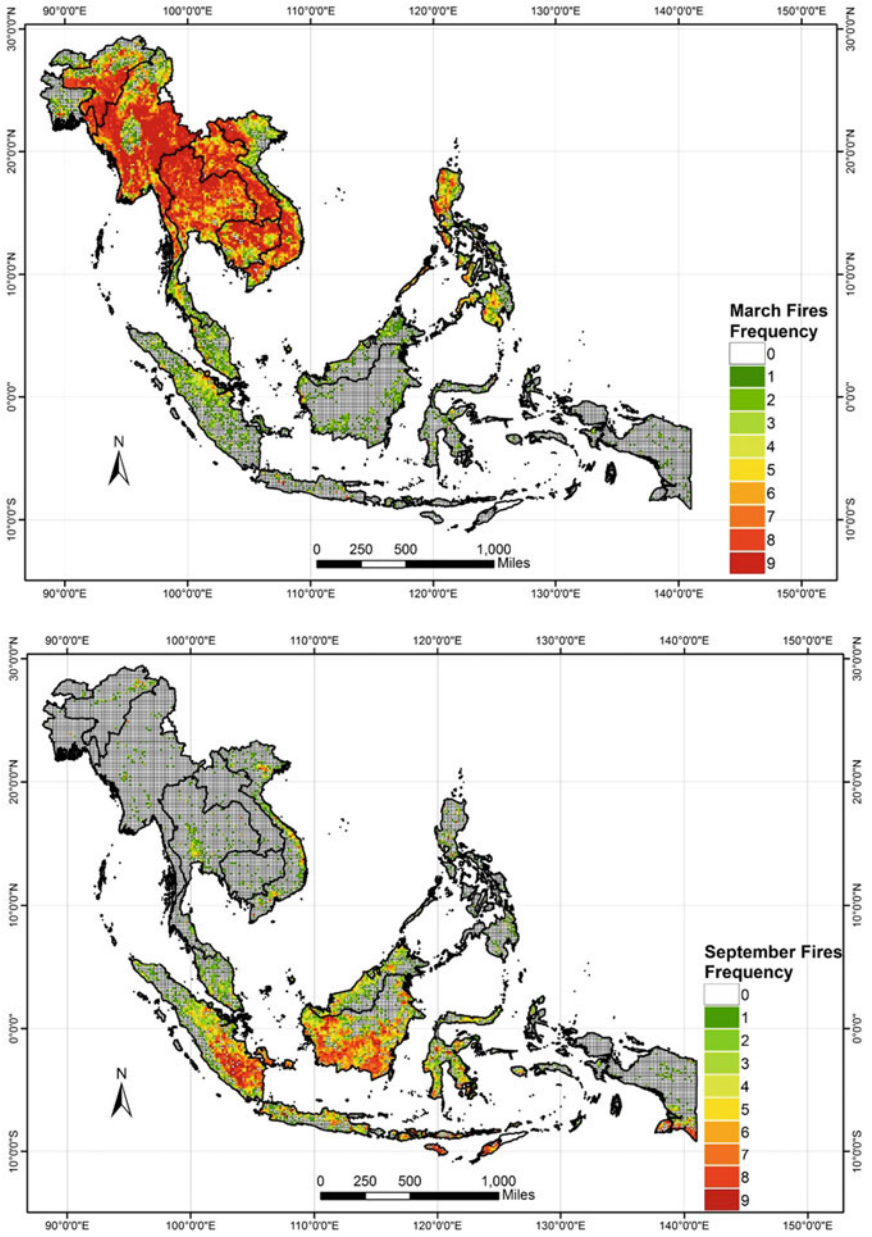

Fig. 6 **a** Spatial variation in fire frequencies in southeast Asia for the month of March and September (2003–2011). **b** A clear north–south gradient in fire frequencies and seasonality was observed in the region

Table 2 Monthly MOPITT surface CO (ppbv) statistics for 0.5 × 0.5 km^2 grid cells obtained from averaging 2002–2010 datasets over the South Asia region

Months	Minimum	Maximum	Mean	St. Dev
Jan	0	567.04	164.38	117.25
Feb	0	570.07	182.52	118.67
Mar	80.34	704.58	271.7	129.07
Apr	0	625.6	159	117.1
May	0	388.83	120.27	77.06
Oct	0	529.21	118.3	85.25
Nov	0	423.65	124.08	90.72
Dec	0	548.81	148.15	120.83

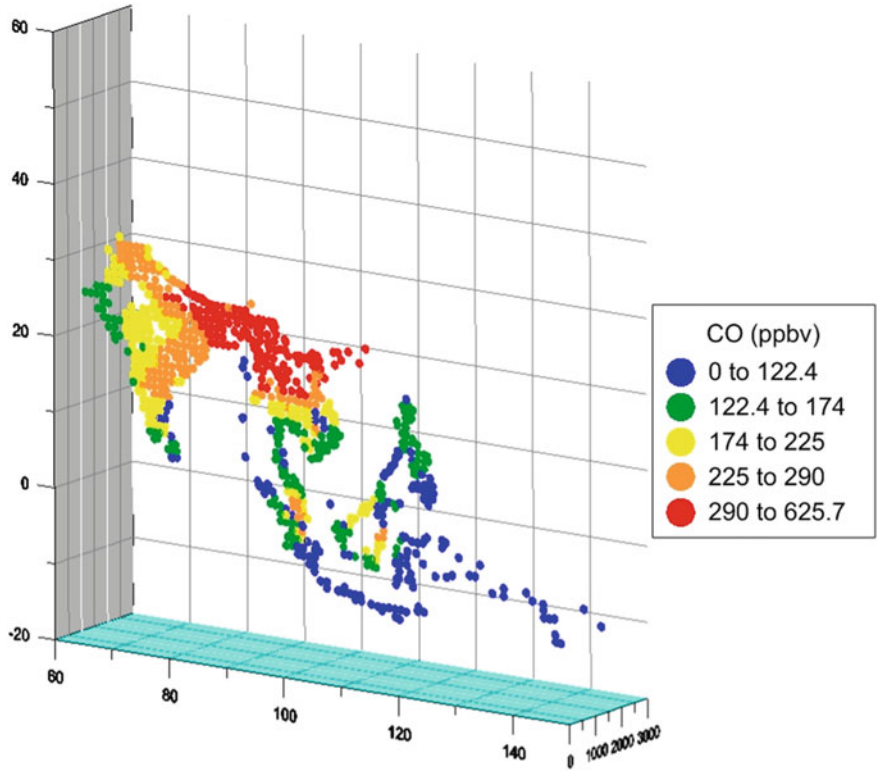

Fig. 7 MOPITT CO (ppbv) concentrations during the peak biomass burning month of March (2010)

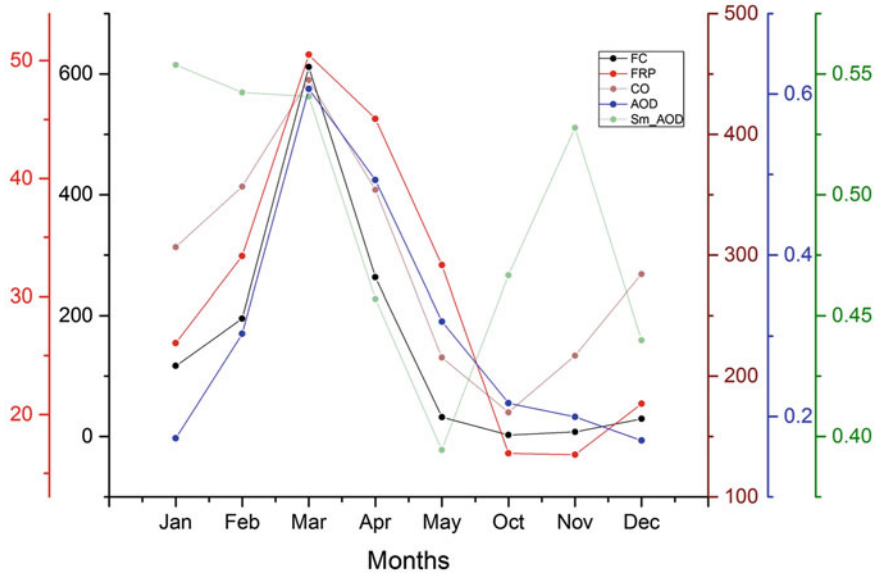

Fig. 8 Variations in fire counts, FRP (MW), CO (ppbv), AOD and small mode AOD in southeast Asia during the peak biomass burning months (2010). The values are mean per 9.3 km^2 grid cells averaged across southeast Asia

We observed a clear increase in "goodness of fit" and adjusted R^2 using the locally weighted regression approach compared to the OLR. For example, during the peak biomass burning month of March, fire counts versus CO using OLR showed r^2 of 0.37 while locally weighted regression showed r^2 of 0.82, almost 45 % increase in correlation and explanation of variance. Among the fire counts and FRP, the correlation strength varied for individual months, however, the relationship was strong and highly significant with both variables ($P < 0.001$) suggesting that either fire counts or FRP can be used as predictor of CO concentrations (Table 3). For example, for the peak biomass burning month of March, fire counts could explain 81 % of variance, whereas FRP could explain 77 %. For other months of January, February and April, both the fire counts and FRP had almost similar adjusted r^2.

Spatial correlation maps of Fire–CO and FRP–CO relationships suggested highest correlation over northeast India and Southeast Asia countries of Myanmar, Thailand, Laos, Vietnam, etc. The lowest correlation was evident over Rajasthan desert regions which didn't have fires and also over Pakistan, Afghanistan, west coast of India with very few fire counts, thus low CO concentrations. The fire counts versus CO and FRP versus CO spatial correlations were consistent with the location and intensity of MODIS fires. In general, when solving for emissions within a selected region or a grid cell, contribution from outside such as through long range transport needs addressing such as through 3D atmospheric transport modeling (Pfister et al. 2005; Stohl 2002). Even without transport modeling, using

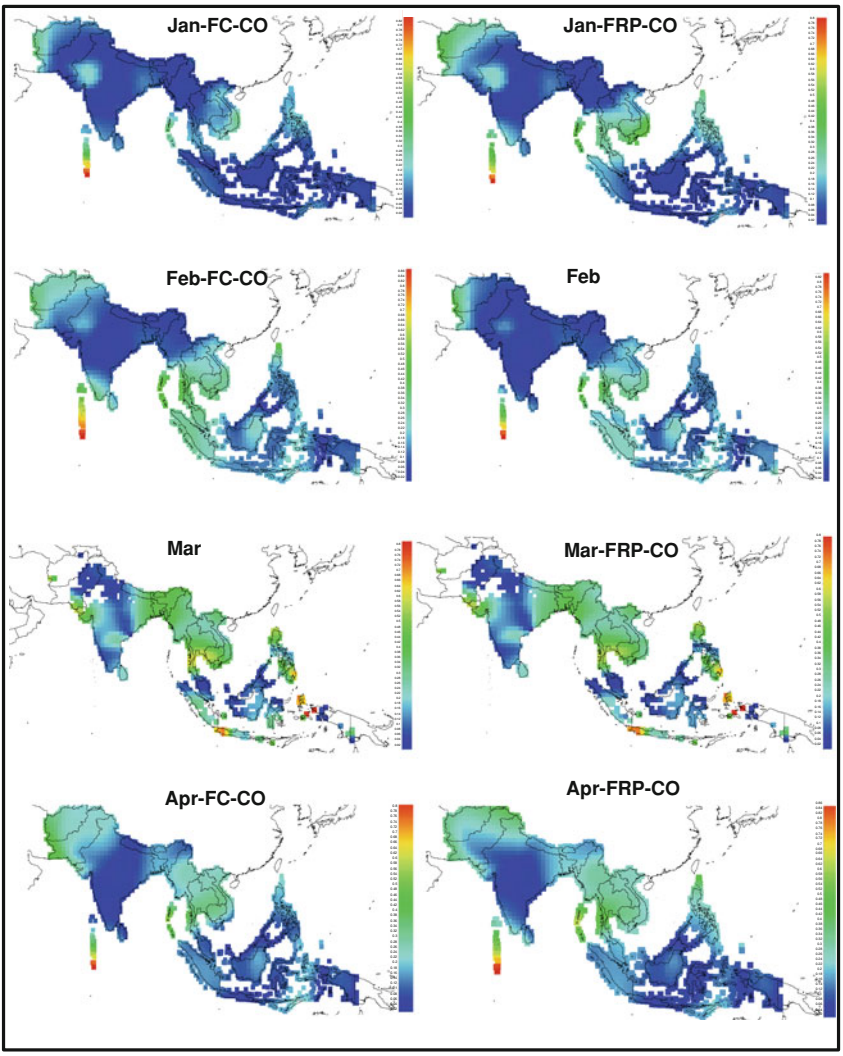

Fig. 9 **a** Spatial correlations between MODIS fire counts (FC), FRP and CO for individual months at 0.5 × 0.5 degree grid cells. **b** The correlation values from ordinary least square regression (OLR) and local regression are shown in Table 3

the locally weighted regression approach, we could explain 80 % of variance in CO datasets from fires during the peak biomass burning months. Our analysis clearly suggests biomass burning influence on CO concentrations, both spatially and temporally in the Asian region. Further, we used surface CO retrievals from MOPITT that are more representative of surface processes and emission sources in

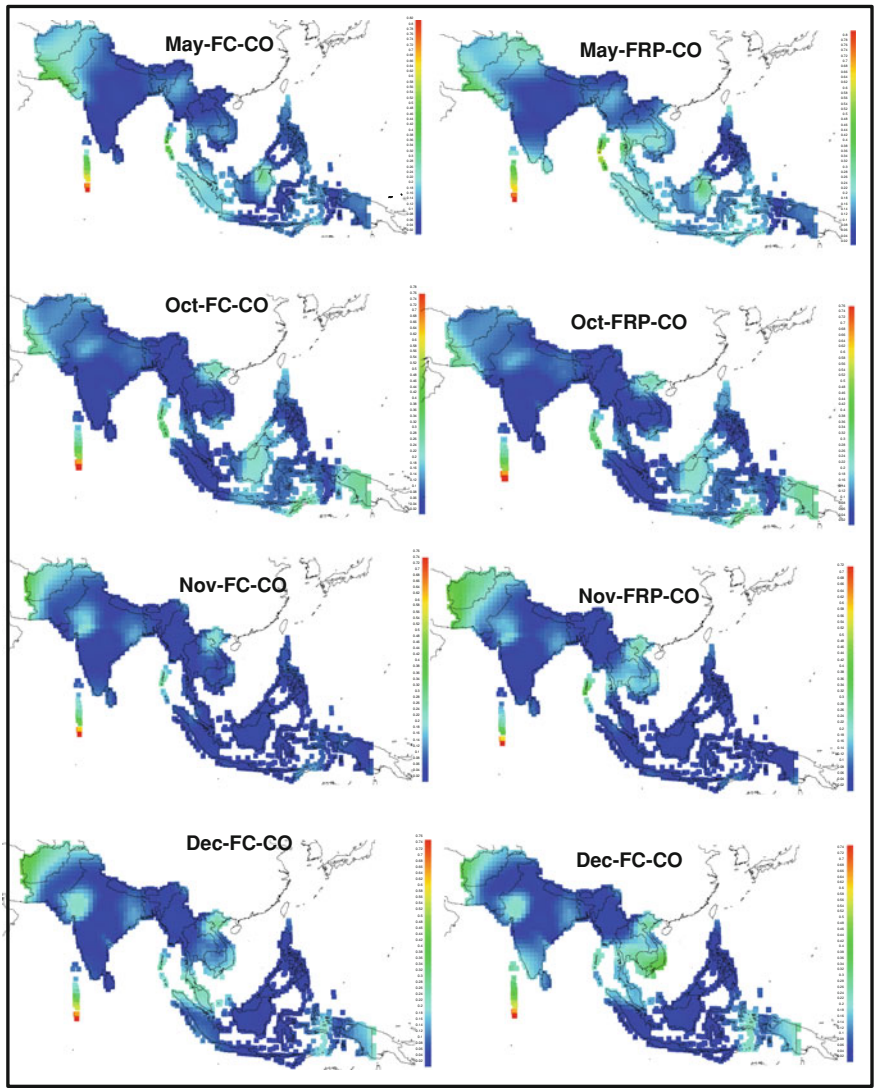

Fig. 9 continued

contrast to the total columnar measurements. Thus, our results also highlight the potential of surface level CO retrievals from MOPITT in capturing spatial and temporal variations and fire episodic events. In contrast, more work is needed to resolve discrepancies in SMAF variations and its' relationship with biomass burning and other emission sources.

Table 3 Regression results from (a) fire counts as predictor and CO as response variable for South Asia (b) FRP as predictor and CO as response variable for South Asia

Months	Correlation coefficient (r)	Coefficient of determination (r^2)	Adjusted r-square	*P*-value
(a)				
Jan	0.838 (0.167)	0.702 (0.028)	0.697 (0.028)	<0.001
Feb	0.834 (0.367)	0.696 (0.135)	0.69 (0.135)	<0.001
Mar	0.90 (0.60)	0.822 (0.37)	0.817 (0.37	<0.001
Apr	0.834 (0.429)	0.696 (0.184)	0.691 (0.184)	<0.001
May	0.758 (0.209)	0.575 (0.044)	0.568 (0.044)	<0.001
Oct	0.623 (0.09)	0.388 (0.008)	0.377 (0.008)	<0.001
Nov	0.8 (0.09)	0.64 (0.008)	0.634 (0.008)	<0.001
Dec	0.874 (0.182)	0.764 (0.033)	0.759 (0.033)	<0.001
(b)				
Jan	0.846 (0.335)	0.715 (0.112)	0.709 (0.112)	<0.001
Feb	0.84 (0.422)	0.705 (0.178)	0.699 (0.178)	<0.001
Mar	0.886 (0.374)	0.786 (0.14)	0.777 (0.14)	<0.001
Apr	0.842 (0.562)	0.709 (0.315)	0.703 (0.315)	<0.001
May	0.772 (0.386)	0.595 (0.149)	0.587 (0.149)	<0.001
Oct	0.633 (0.184)	0.401 (0.034)	0.389 (0.034)	<0.001
Nov	0.801 (0.061)	0.641 (0.004)	0.634 (0.004)	<0.001
Dec	0.876 (0.232)	0.768 (0.054)	0.763 (0.054)	<0.001

The standard OLS values are shown in parenthesis along with the local regression values. Results for June, July and August are not presented as most of the region is impacted by cloud cover

Acknowledgements The authors would like to thank Dr. Louis Giglio (UMd) for the MODIS active fire data set and CMG product used in this study. This research was supported by NASA grant NNX10AU77G.

References

Bonnett S, Gariavait S (2011) Seasonal variability of biomass open burning activities in the greater mekong sub-region. In: Tsuruta H, Fukuyama K (eds) Biomass burning and impacts impacts on Earth's environment vol 15(1). Global Environmental Research, pp 31–37

Bose S (2012) Increases and decreases in the fine mode fraction of aerosol optical depth with increasing relative humidity. Univ Illinois Urbana-Champaign: Thesis. http://hdl.handle.net/2142/29662

Burrows JP, Platt U, Borrell P (2011) The remote sensing of tropospheric composition from space. Springer, New York

Chan LY, Chan CY, Liu HY, Christopher S, Oltmans SJ, Harris JM (2000) Case study on the biomass burning in Southeast Asia and enhancement of tropospheric ozone over Hong Kong. Geophys Res Lett 27(10):1479–1482

Chang D, Song Y (2010) Estimates of biomass burning emissions in tropical Asia based on satellite-derived data. Atmos Chem Phys 10:2335–2351

Cleveland WS, Devlin SJ (1988) Locally weighted regression: an approach to regression analysis by local fitting. J Am Stat Assoc 83(403):596–610

Deeter MN, MOPITT Algorithm Development Team (2009) MOPITT (measurements of pollution in the troposphere) validated version 4 product user's guide. http://www.acd.ucar.edu/mopitt/v4_users_guide_val.pdf

Deeter MN, Emmons LK, Francis GL, Edwards DP, Gille JC, Warner JX, Khattatov B, Ziskin D, Lamarque JF, Ho SP, Yudin V, Attie JL, Packman D, Chen J, Mao D, Drummond JR (2003) Operational carbon monoxide retrieval algorithm and selected results for the MOPITT instrument. J Geophys Res 108(D14):4399. doi:10.1029/2002JD003186

Dennis RA, Mayer J, Applegate G (2005) Fire, people and pixels: linking social science and remote sensing to understand underlying causes and impacts of fires in Indonesia. Hum Ecol 33:465–504

Drummond JR (1992) Measurements of pollution in the troposphere (MOPITT). In: Gille JC, Visconti G (eds) The use of EOS for studies of atmospheric physics. New York, North-Holland, pp 77–101

Fotheringham A, Brunsdon SC, Charlton M (2002) Geographically weighted regression. Wiley, New York

Fu JS, Hsu NC, Gao Y, Huang K, Li C, Lin NH, Tsay SC (2012) Evaluating the influences of biomass burning during 2006 BASE-ASIA: a regional chemical transport modeling. Atmos Chem Phys 12:3837–3855

Gadde B, Bonnet S, Menke C, Garivait S (2011) Air pollutant emissions from rice straw open field burning in India, Thailand and the Philippines. Environ Pollut 157(5):1554–1558

Giglio L, Descloitres J, Justice CO, Kaufman Y (2003) An enhanced contextual fire detection algorithm for MODIS. Remote Sens Environ 87:273–282

Giglio L, Csiszar I, Justice CO (2006) Global distribution and seasonality of active fires as observed with the terra and aqua moderate resolution Imaging spectroradiometer (MODIS) sensors. J Geophys Res 111(G2):G02016

Hoelzemann JJ, Schultz MG, Brasseur GP, Granier C, Simon M (2004) Global wildland fire emission model (GWEM): evaluating the use of global area burnt satellite data. J Geophys Research 109(D14):D14S04

Hooijer A, Page S, Jauhiainen J, Lee WA, Lu XX, Idris A, Anshari G (2012) Subsidence and carbon loss in drained tropical peatlands. Biogeosciences 9(3):1053–1071

Hsu NC, Herman JR, Tsay SC (2003) Radiative impacts from biomass burning in the presence of clouds during boreal spring in Southeast Asia. Geophys Res Lett 30(5):1224

Huang Y, Leung Y (2002) Analyzing regional industrialization in Jiangsu province using geographically weighted regression. J Geogr Syst 4(2):233–249

Ichoku C, Giglio L, Wooster MJ, Remer LA (2008) Global characterization of biomass-burning patterns using satellite measurements of fire radiative energy. Remote Sens Environ 112(6):2950–2962

Jaenicke J, Rieley JO, Mott C, Kimman P, Siegert F (2008) Determination of the amount of carbon stored in Indonesian peatlands. Geoderma 147:151–158. doi:10.1016/j.geoderma.2008.08.008

Kaiser JW, Heil A, Andreae MO, Benedetti A, Chubarova N, Jones L, Morcrette JJ, Razinger M, Schultz MG, Suttie M, van der Werf GR (2012) Biomass burning emissions estimated with a global fire assimilation system based on observed fire radiative power. Biogeosciences 9(1):527–554

Kaufman YJ, Justice CO, Flynn L, Kendall JD, Prins EM, Giglio L, Ward D, Menzel W, Setzer A (1998) Potential global fire monitoring from EOS-MODIS. J Geophys Res 103(D24):32215–32238

Kimothi MM, Jadhav RN (1998) Forest fire in the Central Himalaya: an extent direction and spread using IRS LISS-I data. Int J Remote Sens 19(12):2261−2274

Kopacz M, Jacob DJ, Fisher JA, Logan JA, Zhang L, Megretskaia IA, Yantosca RM, Singh K, Henze DK, Burrows JP, Buchwitz M, Khlystova I, McMillan WW, Gille JC, Edwards DP, Eldering A, Thouret V, Nedelec P (2010) Global estimates of CO sources with high resolution by adjoint inversion of multiple satellite datasets (MOPITT, AIRS, SCIAMACHY, TES). Atmos Chem Phys 10(3):855–876

Lau WKM, Kim MK, Kim KM, Lee WS (2010) Enhanced surface warming and accelerated snowmelt in the Himalayas and Tibetan Plateau induced by absorbing aerosols. Environ. Res. Lett 5(2):025204. doi:10.1088/1748-9326/5/2/025204

Levy RC, Remer LA, Mattoo S, Vermote EF, Kaufman YJ (2007) Second-generation operational algorithm: retrieval of aerosol properties over land from inversion of moderate resolution imaging spectroradiometer spectral reflectance. J Geophys Res 112(D13):D13211

Li H, Han Z, Cheng T, Du H, Kong L, Chen J, Zhang R, Wang W (2010) Agricultural fire impacts on the air quality of Shanghai during summer harvest time. Aerosol Air Quality Res 10(2):95–101

Miettinen J, Shi C, Liew SC (2011) Deforestation rates in insular Southeast Asia between 2000 and 2010. Glob Change Biol 17(7):2261–2270

Monks PS, Beirle S (2011) Applications of satellite observations of tropospheric composition. In: Burrows JP, Platt U, Borrell P (eds) The remote sensing of tropospheric composition from space. Springer, Berlin, pp 365–449

Montzka SA, Krol M, Dlugokencky E, Hall B, Jöckel P, Lelieveld J (2011) Small interannual variability of global atmospheric hydroxyl. Science 331(6013):67–69

Murdiyarso D, Adiningsih ES (2007) Climate anomalies, Indonesian vegetation fires and terrestrial carbon emissions. Mitig Adapt Strat Glob Change 12(1):101–112

Nawahda A, Yamashita K, Ohara T, Kurokawa J, Yamaji K (2012) Evaluation of premature mortality caused by exposure to PM 2.5 and Ozone in East Asia: 2000, 2005, 2020. Water Air Soil Pollut 223:1–15

Page SE, Sigert F, Rieley JO, Boehm HDV, Jaya A, Limin S (2002) The amount of carbon released from peat and forest fires in Indonesia during 1997. Nature 420(6911):61−65

Page S, Hoscilo A, Langner A, Tansey K, Siegert F, Limin S, Rieley J (2009) Tropical peatland fires in Southeast Asia. Trop Fire Ecol, 263–287

Page SE, Rieley JO, Banks CJ (2011) Global and regional importance of the tropical peatland carbon pool. Glob Change Biol 17(2):798−818

Pfister G, Hess PG, Emmons LK, Lamarque J-F, Wiedinmyer C, Edwards DP, Pétron G, Gille JC, Sachse GW (2005) Quantifying CO emissions from the 2004 Alaskan wildfires using MOPITT CO data. Geophys Res Lett 32:L11809. doi:10.1029/2005GL022995

Pope CA III, Dockery DW (2006) Health effects of fine particulate air pollution: lines that connect. J Air Waste Manag Assoc 56(6):709–742

Prasad KV, Badarinath KVS, Anuradha E (2008) Biophysical and anthropogenic controls of forest fires in the Deccan Plateau, India. J Environ Manag 86:1–13

Radojevic M (2003) Chemistry of forest fires and regional haze with emphasis on Southeast Asia. Pure appl Geophys 160(1):157–187

Ramanathan V, Chung C, Kim D, Bettge T, Buja L, Kiehl JT, Washington WM, Fu Q, Sikka DR, Wild M (2005) Atmospheric brown clouds: impacts on South Asian climate and hydrological cycle. Proc Natl Acad Sci USA 102(15):5326-5333

Ramanathan V, Carmichael G (2008) Global and regional climate changes due to black carbon. Nat Geosci 1(4):221–227

Remer L et al (2005) The MODIS aerosol algorithm, products, and validation. J Atmos Sci 62(4):947–973

Seaton A, Godden D, MacNee W, Donaldson K (1995) Particulate air pollution and acute health effects. The Lancet 345(8943):176–178

Stohl A, Eckhardt S, Forster C, James P, Spichtinger N (2002) On the pathways and timescales of intercontinental air pollution transport. J Geophys Res 107(D23):4684. doi:10.1029/2001JD001396

Streets DG, Yarber KF, Woo J-H, Carmichael GR (2003) Biomass burning in Asia: annual and seasonal estimates and atmospheric emissions. Global Biogeochem Cycles 17(4):1099. doi:10.1029/2003GB002040

Sugi K, Theissen JL, Traber LD, Herndon DN, Traber DL (1990) Impact of carbon monoxide on cardiopulmonary dysfunction after smoke inhalation injury. Circ Res 66(1):69–75

Vadrevu KP, Badarinath KVS (2009) Spatial pattern analysis of fire events in central India—a case study. Geocarto Int 24(2):115–131

Vadrevu KP, Anuradha E, Badarinath. KVS (2010) Fire risk evaluation using multi-criteria analysis—A case study. Environ Monitoring Assess 166(1–4):223–239. doi:10.1007/s10661-009-0997-3

Vadrevu KP, Ellicott E, Badarinath KVS, Vermote E (2011) MODIS derived fire characteristics and aerosol optical depth variations during the agricultural residue burning season, North India. Environ Pollut 159(6):1560–1569

Vadrevu KP, Ellicott E, Giglio L, Badarinath KVS, Vermote E, Justice C, Lau KW (2012a) Vegetation fires in the Himalayan region—aerosol load, black carbon emissions and smoke plume heights. Atmos Environ 47:241–251

Vadrevu KP, Csiszar I, Ellicott E, Giglio L, Badarinath KVS, Vermote E, Justice C (2012b) Hotspot Analysis of Vegetation Fires and Intensity in the Indian Region. IEEE J Sel Top Appl Earth Obs Remote Sens 99:1–15

Vadrevu KP, Giglio L, Justice C (2013) Satellite-based analysis of fire–CO relationships from forest and agriculture residue burning (2003–2011). Atmos Environ. doi:10.1016/j.atmosenv.2012.09.055

Van der Werf GR, Randerson JT, Giglio L, Collatz GJ, Kasibhatla PS, Arellano AF Jr (2006) Interannual variability in global biomass burning emissions from 1997–2004. Atmos Chem Phys 6:3423–3441. doi:10.5194/acp-6-3423

Wooster MJ, Zhang YH (2004) Boreal forest fires burn less intensely in Russia than in North America. Geophys Res Lett 31(L20505):10–1029

Wooster MJ, Roberts G, Perry GLW, Kaufman YJ (2005) Retrieval of biomass combustion rates and totals from fire radiative power observations: FRP derivation and calibration relationships between biomass consumption and fire radiative energy release. J Geophys Res 110:D24311–D24311

Zhang L, Li QB, Jin J, Liu H, Livesey N, Jiang JH, Mao JH, Chen D, Luo M, Chen Y (2011) Impacts of 2006 Indonesian fires and dynamics on tropical upper tropospheric carbon monoxide and ozone. Atmos Chem Phys 11:10929–10946